Liquid Crystals
Publication details, including instructions for authors and subscription information:
http://www.informaworld.com/smpp/title~content=t713926090

Calorimetric study on the thermotropic cubic mesogen, 4'-n-hexadecyloxy-3'-nitrobiphenyl-4-carboxylic acid, ANBC(16)

Ayako Sato

Online publication date: 06 August 2010

To cite this Article Sato, Ayako(1999) 'Calorimetric study on the thermotropic cubic mesogen, 4'-n-hexadecyloxy-3'-nitrobiphenyl-4-carboxylic acid, ANBC(16)', Liquid Crystals, 26: 3, 341 — 349
To link to this Article: DOI: 10.1080/026782999205119
URL: http://dx.doi.org/10.1080/026782999205119

LIQUID CRYSTALS, 1999, VOL. 26, NO. 3, 341–349

Calorimetric study on the thermotropic cubic mesogen, 4′-*n*-hexadecyloxy-3′-nitrobiphenyl-4-carboxylic acid, ANBC(16)†

AYAKO SATO, KAZUYA SAITO and MICHIO SORAI*

Microcalorimetry Research Center, School of Science, Osaka University, Toyonaka, Osaka 560-0043, Japan

(*Received 13 July 1998; accepted 9 October 1998*)

The heat capacity of ANBC(16) has been measured between 15 and 500 K by adiabatic calorimetry. Three (one known and two newly found) crystal–crystal phase transitions and all the known liquid crystalline phases (SmC, cubic D and SmA) were detected. The temperatures, enthalpies and entropies of transition were determined for all the phase transitions observed. The entropy of transition is very small for the transition from/to the cubic D mesophase. The results are compared with the thermal properties of another cubic mesogen, BABH(8). The logical possibility is pointed out that the cubic mesophases of ANBC(16) and BABH(8) are of identical higher order structure, while discussing the fact that they are immiscible.

1. Introduction

In 1957 an exotic liquid crystalline phase was discovered in a series of ANBC(n_C) (4′-*n*-alkoxy-3′-nitrobiphenyl-4-carboxylic acids, n_C: the number of carbon atoms in the alkoxy chain) [1]. This mesophase was optically isotropic and was classified as the SmD phase. Since a layered smectic structure is inconsistent with isotropy, this phase is nowadays called the 'D phase'. Since then increasing attention has been focused on its structure and stability [2, 3]. The molecule of ANBC consists of a nitrobiphenylcarboxylic acid core and an *n*-alkoxy chain as shown in figure 1. Since, however, most molecules are dimerized in the solid and liquid crystalline phases [4, 5] via intermolecular hydrogen bonds, the system consists of a 'molecule' that has a long core at its centre and two terminal alkoxy chains.

Two structural models of the D phase have been proposed. One assumes an ordered packing of spherical micelles [6] and the other is called the interwoven jointed-rod model [7–12]. Nowadays, the latter is commonly accepted on the basis of experimental results obtained by X-ray diffraction [11], NMR spectroscopy [5, 13] and dynamic viscoelastic measurements [14]. The establishment of the structural model is, however, not a goal, but a starting point for obtaining a microscopic understanding of the stability of the peculiar aggregation style of the molecules of the D phase. Since reliable thermodynamic data are crucial to proposing a concrete framework for possible statistical models and also to discriminate good statistical models, the present authors started thermodynamic studies on liquid crystalline phases of cubic symmetry [15–21].

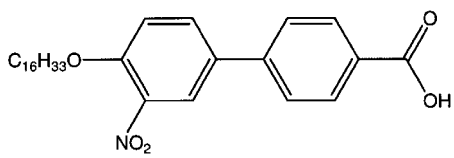

ANBC(16)

Figure 1. Structure of ANBC(16) molecule.

In the first paper [19] in this series of studies, the phase diagrams of the binary systems, ANBC(n_C)–*n*-tetradecane (n_C = 8, 16 and 18), was studied while paying special attention to the roles of the molecular core and the terminal chains in relation to the thermodynamic stability of the D phase. The results showed that the apparent dependence on the number of paraffinic carbon atoms in the system bears a resemblance to the n_C dependence in the homologous series of ANBC(n_C), implying that the terminal alkoxy chains, at least in the D phase, behave like the solvent in lyotropic liquid crystals. The minimum size of the 'molecular core' necessary for stabilizing the D phase was also suggested.

The second and third papers [20, 21] reported the thermodynamic properties of BABH(8) [1,2-bis-(4-*n*-octyloxybenzoyl)hydrazine], which shows another isotropic liquid crystal phase called simply 'cubic phase' [22, 23]. The results [20] showed that the entropy of transition between the cubic and SmC phases is very small in spite of the large difference between their possible structures.

*Author for correspondence.

†Contribution No. 150 from the Microcalorimetry Research Center.

Journal of Liquid Crystals ISSN 0267-8292 print/ISSN 1366-5855 online
http://www.tandf.co.uk/JNLS/lct.htm
http://www.taylorandfrancis.com/JNLS/lct.htm

This paper is the fourth in the series. Precise heat capacity measurements have been made on the first cubic mesogen ANBC(16) which has the longest history of study. This compound is known to show the following phase sequence on heating from the crystalline phase [1, 3, 24]: room temperature crystal → high temperature crystal → SmC phase → D phase → SmA phase → isotropic liquid. In this paper, the results of the heat capacity measurements, including the thermodynamic properties of the phase transitions, are reported in detail.

2. Experimental

The specimen of ANBC(16) was synthesized according to the method reported [1], starting from 4′-hydroxybiphenyl-4-carboxylic acid (Aldrich Chemicals), 1-bromohexadecane (Wako Pure Chemicals) and fuming nitric acid (Wako Pure Chemicals), and purified by repeated recrystallization from ethanol. The quality of the sample was checked by elemental analysis, ^{1}H NMR, and mass-spectrometry, which showed no impurities. The purity of the specimen used for calorimetry was finally determined as 99.6 mol % by a fractional melting method as described below. The sample was dried in a vacuum before loading into a calorimeter vessel. To avoid direct contact between the sample and the wall of the gold-plated beryllium-copper vessel, the sample was loaded into a quartz glass beaker with a lid (5.7 g in mass), which was put in the vessel. A small amount of helium gas was sealed within the vessel (26 kPa at room temperature) to assist thermal equilibration. The mass of the sample loaded was 3.3789 g (6.9866 mmol) after buoyancy correction. The sample contributed about 20% to the total heat capacity including that of the calorimeter vessel and that of the quartz glass beaker in the normal temperature range.

The thermometer mounted on the calorimeter vessel was a platinum resistance thermometer (Minco Product, S1059), whose temperature scale was based upon the IPTS-68. The details of the adiabatic calorimeter, the operation and procedure for heat capacity measurement were described in detail elsewhere [25].

To establish the temperature dependence of the heat capacity above the transition to the isotropic liquid, a commercial DSC instrument (Perkin Elmer DSC-7) was employed because use of the adiabatic calorimetry was so time consuming (about 70 min per data point) that the sample decomposed slowly during the long exposure to high temperature. In contrast, DSC at a rapid scan rate (5 K min^{-1}) gave completely reproducible thermograms, implying no decomposition.

3. Results and discussion

3.1. *Heat capacity, excess enthalpy and entropy, and thermodynamic functions*

The heat capacity of ANBC(16) was measured between 13 and 483 K by adiabatic calorimetry. The primary data for the heat capacities are in table 1 and typical data are shown in figure 2 for the whole temperature range studied. The time needed for thermal equilibration was 20 min below 30 K, 30 min at 100 K, 20 min at 200 K and 30 min above 300 K, outside the transition region. These are typical for this adiabatic calorimeter independently of samples. In the transition region, however, the thermal relaxation time was significantly and abruptly prolonged when the transition temperature was approached. The longest time used for monitoring the temperature drift was, however, 120 min in these experiments for practical reasons. This truncation obviously has an influence on the resulting data for apparent heat capacity, but no effect on the integrated enthalpy change because of the first law of thermodynamics. In reality, since the transitions are first order, the temperature interval is narrow where the time required for thermal equilibration is significantly longer than 120 min. The accuracy of the resultant excess enthalpy and entropy mostly depends on the uncertainty involved in drawing a baseline.

The melting temperature of ANBC(16) is known to be about 400 K [1, 24]. Indeed the largest anomaly due to the transition between the crystalline phase and the SmC phase is located at 401.12 K with an enthalpy gain of 38.92 kJ mol^{-1}. The purity of the sample was determined by means of the fractional melting method, which utilizes melting point depression. In the analysis, unknown impurities were assumed to be soluble in the

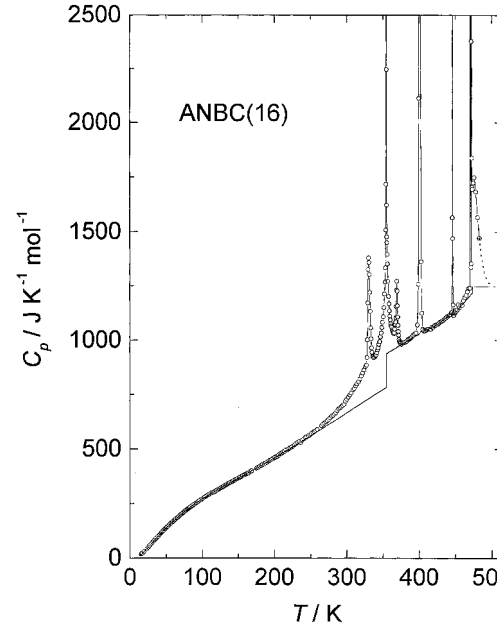

Figure 2. Measured molar heat capacities of ANBC(16) in the whole temperature region studied. The baselines for separating the excess heat capacities are also drawn.

Table 1. Measured molar heat capacity of ANBC(16).

T	$C_{p,\mathrm{m}}$	T	$C_{p,\mathrm{m}}$	T	$C_{p,\mathrm{m}}$	T	$C_{p,\mathrm{m}}$
K	J K^{-1} mol^{-1}	K	J K^{-1} mol^{-1}	K	J K^{-1} mol^{-1}	K	J K^{-1} mol^{-1}
Series 1		168.279	401.44	294.168	699.93	57.935	165.70
79.663	225.23	174.804	413.12	296.050	706.00	59.456	170.24
81.232	229.13	176.951	417.45	297.934	718.93	61.008	174.54
82.769	233.16	179.084	421.04	299.917	728.71	62.560	178.22
84.278	236.77	181.204	425.15	302.001	738.25	64.116	183.30
85.759	240.39	183.311	429.01	304.078	747.78	65.623	187.47
87.216	243.59	185.406	433.03	306.149	756.80	67.118	191.61
88.649	247.01	187.489	435.85	308.212	771.04	68.601	195.89
90.061	250.09	189.562	440.25	310.266	778.34	70.047	199.83
91.623	253.72	191.624	444.84	312.311	789.59	71.457	203.85
93.332	257.85	193.674	449.15	314.348	800.41	72.836	207.54
95.013	261.44	195.714	452.51	316.369	832.60	74.186	211.24
96.668	265.22	197.743	456.64	318.380	827.03	75.508	214.68
98.299	268.71	199.762	460.69	320.387	840.15	76.805	218.10
99.907	272.74	201.772	464.22	322.384	854.57	78.078	221.52
101.493	276.47	203.772	467.36	324.371	868.78	79.329	224.77
103.059	280.18	205.763	472.55	326.342	903.08	80.560	227.91
104.605	283.75	207.743	479.70	328.252	1075.3	81.772	230.84
106.133	287.34	209.714	480.74	330.038	1344.2	82.965	233.94
107.644	290.32	211.677	484.93	331.780	1233.0	84.202	237.01
109.139	293.11	213.632	488.88	333.594	1059.0	85.481	239.96
110.618	295.91	215.576	496.55	335.478	968.69	86.741	242.90
112.082	298.34	217.512	496.50	337.396	941.82	87.984	246.18
113.676	300.89	219.441	500.93	339.322	939.27		
115.396	303.24	221.363	504.92	341.246	951.36	*Series 3*	
117.098	305.45	223.276	509.08	343.159	970.53	314.045	799.36
118.782	309.61	225.319	511.63			316.046	809.92
120.449	312.77	227.492	517.48	*Series 2*		318.038	823.00
122.100	315.62	229.653	524.84	15.396	18.350	320.018	837.17
123.736	318.99	231.803	529.35	16.304	21.540	321.988	850.32
125.357	322.28	233.944	533.88	17.272	23.703	323.949	864.30
126.963	325.41	236.081	529.20	19.508	30.025	325.899	879.24
128.557	328.31	238.211	540.92	23.661	44.464	327.196	886.72
130.137	331.60	240.327	546.82	25.088	50.125	327.842	921.05
131.705	334.62	242.432	553.25	26.547	56.375	328.477	1003.1
133.260	337.37	244.526	556.05	28.007	61.658	329.084	1170.8
134.804	340.37	246.614	560.57	29.518	67.532	329.656	1326.5
136.337	343.27	248.694	564.24	31.063	73.437	330.207	1380.4
137.859	345.99	250.767	569.16	32.582	78.603	330.753	1358.9
139.371	348.41	252.830	574.37	34.086	84.569	331.305	1304.0
140.873	351.15	254.886	580.04	35.547	89.695	331.871	1220.7
142.365	353.46	256.934	584.48	36.901	94.577	332.453	1133.6
143.848	357.00	258.973	590.08	38.167	99.037	333.051	1057.2
145.323	359.02	265.035	607.73	39.361	103.24	333.664	1007.6
146.788	361.90	267.041	613.64	40.491	107.56	334.287	966.26
148.246	364.27	269.040	619.63	41.568	111.16	334.918	945.77
149.695	368.38	271.031	625.32	42.598	114.68	335.553	926.59
151.136	370.40	273.013	631.27	43.586	118.28	336.358	925.11
152.569	372.60	274.987	636.75	44.536	121.47	337.331	920.00
153.994	375.73	276.950	643.72	45.673	125.47	338.370	923.28
155.411	378.89	278.901	650.82	46.982	129.89	339.474	928.44
156.821	381.38	280.840	655.51	48.233	134.46	340.574	936.45
158.223	382.81	282.774	662.48	49.434	138.51	341.670	947.92
159.620	385.76	284.706	667.04	50.589	142.42	342.762	962.22
161.009	388.05	286.631	676.70	51.804	146.25	343.848	981.50
162.392	389.71	288.542	685.23	53.280	151.35	344.928	991.67
163.769	391.21	290.435	690.21	54.896	156.42	346.003	1011.2
166.501	397.86	292.301	694.97	56.445	161.42	347.071	1030.0

Table 1. (*continued*).

T	$C_{p,m}$	T	$C_{p,m}$	T	$C_{p,m}$	T	$C_{p,m}$
K	J K^{-1} mol^{-1}	K	J K^{-1} mol^{-1}	K	J K^{-1} mol^{-1}	K	J K^{-1} mol^{-1}
348.130	1055.5	363.527	1041.8	387.551	1008.5	446.456	1829.2
349.181	1084.4	364.180	1037.5	389.164	1014.4	447.359	1253.6
350.222	1120.8	364.833	1031.1	390.774	1022.2	448.341	1127.5
351.250	1160.1	365.486	1035.1	392.382	1025.0	449.339	1126.3
352.264	1227.4	366.137	1052.5	393.986	1031.0	450.337	1134.3
353.013	1289.2	366.783	1074.3	395.588	1034.1	451.334	1134.9
353.500	1420.4	367.305	1073.7	397.179	1070.4		
353.961	1655.0	367.706	1085.1	398.520	1259.2	*Series 7*	
354.430	2524.0	368.104	1104.6	399.543	2112.5	444.047	1127.4
354.839	1715.9	368.499	1155.7	400.256	5941.3	445.044	1127.4
355.306	1448.2	368.885	1230.9	400.625	16119	445.692	1565.7
355.791	1395.1	369.263	1271.9	400.806	30776	445.946	3490.9
356.285	1337.1	369.641	1225.5	400.913	48272	446.203	1470.1
359.264	1129.1	370.025	1158.6	400.986	68258	446.601	1163.2
360.398	1092.0	370.416	1106.9	401.039	91592	447.092	1121.9
		370.814	1069.0	401.081	109271	447.586	1113.6
Series 4		371.216	1040.3	401.118	124953	448.079	1127.7
340.416	932.59	371.621	1023.8	401.156	98688	448.572	1124.0
341.424	943.21	372.029	1007.9	401.447	5430.3	449.066	1126.1
342.429	956.01	372.438	1006.0	402.301	1128.8	449.560	1127.9
343.429	966.44	372.848	992.36	403.469	1125.7	450.053	1137.4
344.425	981.72	374.218	993.32	404.647	1051.2	450.888	1134.3
345.416	993.95			406.062	1044.0	452.066	1139.8
346.401	1015.9	*Series 5*		407.711	1046.4	453.583	1164.2
347.380	1035.0	366.077	1049.1	409.347	1051.7	455.446	1151.3
348.352	1058.9	366.657	1070.1			457.309	1162.4
349.317	1083.5	367.233	1077.4	*Series 6*		459.170	1161.7
350.274	1108.2	367.696	1073.5	406.525	1042.0	461.024	1183.0
351.217	1150.7	368.047	1094.7	407.833	1043.2	462.872	1196.9
352.150	1213.5	368.394	1130.8	409.479	1046.7	464.712	1207.2
352.899	1268.5	368.733	1224.8	411.122	1050.2	466.547	1224.0
353.411	1335.0	369.064	1286.0	412.762	1052.3	468.375	1239.6
353.852	1509.0	369.392	1269.2	414.401	1052.6	469.746	1240.6
354.196	1718.3	369.723	1206.9	416.039	1051.4	470.518	2796.0
354.427	2750.7	370.061	1147.0	417.673	1061.0	471.003	2909.3
354.640	2247.9	370.405	1096.0	419.441	1060.9	471.310	1337.2
354.887	1622.5	370.754	1056.8	421.340	1067.8	471.603	1353.9
355.155	1477.1	371.106	1045.7	423.235	1069.9	471.858	2379.1
355.432	1449.8	371.595	1024.4	427.016	1078.0	472.040	5673.8
355.776	1395.7	372.221	1003.6	428.901	1083.7	472.211	2942.9
356.189	1352.0	372.851	995.75	430.782	1087.3	472.470	1838.5
356.913	1271.9	373.484	990.27	432.660	1091.2	472.788	1705.4
357.741	1202.3	374.118	987.54	434.535	1097.0	473.435	1696.4
358.368	1167.6	375.135	981.97	436.406	1102.8	474.403	1724.4
359.002	1135.5	376.533	987.84	438.273	1108.2	475.850	1749.2
359.640	1111.1	377.931	987.94	440.137	1113.1	477.966	1682.8
360.282	1093.5	379.443	990.51	441.567	1117.1	480.309	1566.1
360.926	1075.9	381.070	992.77	442.566	1118.9	482.733	1471.1
361.574	1065.4	382.694	996.24	443.564	1125.3		
362.223	1059.4	384.315	1002.6	444.562	1128.0		
362.874	1048.9	385.934	1006.3	445.548	1213.6		

liquid crystalline phase (SmC phase), but insoluble in the crystalline phase. The results of the analysis showed that the melting point of pure ANBC(16) is 401.28 K, and the purity of the sample is 99.6 mol %.

In the solid state there are three peaks in the heat capacity curve. The central peak around 355 K is known to be due to a phase transition between crystalline phases [24], while the other two are newly found in the

present experiment. The transition temperatures were determined to be 330.19, 354.43 and 369.22 K as the peak temperatures of the heat capacity curve. In what follows, the crystalline phases will be designated as Cr_1, Cr_2, Cr_3 and Cr_4 on going from high to low temperature. The lowest anomaly at 330.19 K seems to lie on the tail of the middle anomaly at 354.43 K, which extends down to about 250 K. The middle anomaly also has a tail on the high temperature side though its extent is much smaller than that on the low temperature side. The high temperature tail is cut by the highest anomaly at 369.22 K.

To discuss the thermodynamic properties of transitions such as excess enthalpy and entropy, separation of the excess part is necessary. When a transition is first order, the normal heat capacity may jump at the transition temperature. A jump in the heat capacity is clearly recognized between the Cr_4 and Cr_1 phases. This jump must be attributed to some of the three phase transitions. We simply attributed the whole of the jump to the middle transition from Cr_3 to Cr_2 because this transition is by far the largest of the three. The large tail on the low temperature side was separated from the observed values by determining the normal heat capacity on the basis of the effective frequency distribution method [26]. The heat capacity curve thus estimated was used as the baseline for the Cr_4 and Cr_3 phases. For the baseline in Cr_2 and Cr_1, this curve was simply shifted upward until it contacted the observed heat capacity curve in Cr_1. The excess heat capacities thus separated are integrated numerically with respect to T and $\ln T$ to yield the excess enthalpy and entropy, respectively. The entropy acquisition with temperature is shown in figure 3 and the numerical data are given in table 2. The assignment of the excess enthalpy and entropy gains among the phase transitions occurring in the solid state was abandoned because it involves ambiguous assignments of the gain in the tail to each phase transition. The jumps in

Table 2. Thermodynamic quantities associated with thermal anomalies in ANBC(16).

Anomaly	T_{peak} / K	ΔH / kJ mol^{-1}	ΔS / J K^{-1} mol^{-1}
Cr_4–Cr_3 transition	330.19		
Cr_3–Cr_2 transition	354.43	6.59	49.75
Cr_2–Cr_1 transition	369.22		
Cr_1–SmC transition	401.12[a]	38.92	97.08
SmC–D transition	445.95	0.73	1.63
D–SmA transition	470.80	1.90	4.05
SmA–I transition	472.04	2.08	4.40
hump	475	4.65	9.68

[a] Melting point of virtually pure ANBC(16) is 401.28 K.

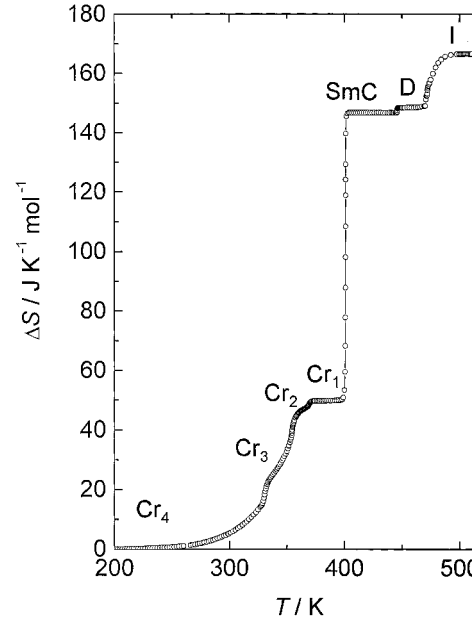

Figure 3. Excess entropy acquisition with temperature of ANBC(16).

enthalpy and entropy are roughly estimated from figure 3 as 2.6 kJ mol^{-1} and 8 J K^{-1} mol^{-1} for the lowest transition at 330.19 K, 4.3 kJ mol^{-1} and 12 J K^{-1} mol^{-1} for the middle transition at 354.43 K, and 0.7 kJ mol^{-1} and 2 J K^{-1} mol^{-1} for the highest transition at 369.22 K.

It is difficult to discuss the properties of each phase transition between the crystalline phases because no information concerning structures and molecular dynamics is available at present. However, since the molecule is large and plausibly does not undergo overall rotation, the large increment in enthalpy and entropy implies the successive conformational disordering of the terminal alkoxy chains. This point will be discussed later in some detail.

The heat capacities above 300 K are shown on an enlarged scale in figure 4. All the known liquid crystalline phases (SmC, D and SmA) are detected. The transition temperatures are 445.95 K for the SmC–D transition, and 470.80 K for the D–SmA transition. These transitions are first order without any remarkable tail on either the low or high temperature sides. The enthalpy gains for these transitions are thus easily determined assuming the normal heat capacity as being represented by quadratic polynomials for the SmC and the D-phases. Since the temperature region where the SmA phase remains stable is very narrow, the normal heat capacity of the SmA phase was assumed to be represented by the extrapolation of that of the D phase. In this way the enthalpy and entropy of transition were determined as 0.73 kJ mol^{-1} and 1.63 J K^{-1} mol^{-1} for the SmC–D transition, and 1.90 kJ mol^{-1} and

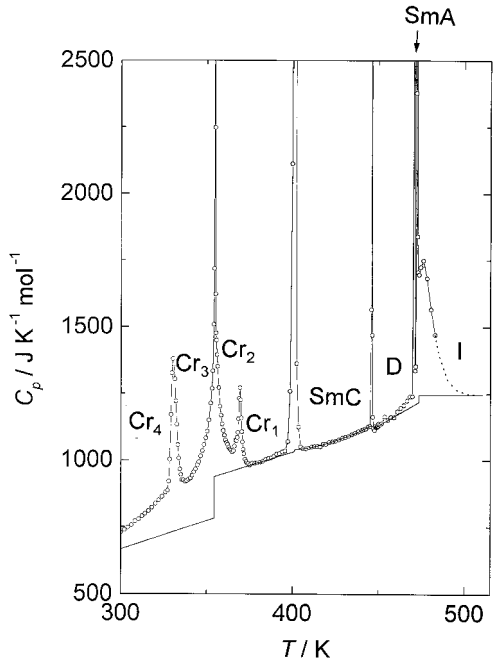

Figure 4. Measured heat capacities of ANBC(16) above 300 K. Extrapolation based on the DSC thermograms is shown by the dotted curve.

4.05 J K^{-1} mol^{-1} for the D–SmA transition, respectively. These data are summarized in table 2 and represented graphically in figure 3.

The heat capacity curve exhibits a remarkable hump above the transition from the SmA phase to the isotropic liquid at 472.04 K. This hump has already been reported in the thermogram in a DSC experiment [24]. Although the separation of this hump and the determination of the enthalpy and entropy of transition for the SmA–isotropic liquid transition require the normal heat capacity of the isotropic liquid, there was a risk that the sample slowly decomposed during the measurement by adiabatic calorimetry because of long exposure to high temperatures. The temperature dependence of the heat capacity was thus determined by DSC. Since the accuracy is much better in adiabatic calorimetry than in DSC, the heat capacity curve determined by adiabatic calorimetry is extrapolated as shown in figure 4 by the dotted curve, on the basis of the DSC thermograms. The heat capacity curve above 506 K is extrapolated linearly to the low temperature to yield the baseline. The enthalpy and entropy associated with the SmA–isotropic liquid transition are determined as 2.08 kJ mol^{-1} and 4.40 J K^{-1} mol^{-1}, respectively. The numerical integration of the hump gives an excess enthalpy gain of 4.65 kJ mol^{-1} and an entropy gain of 9.68 J K^{-1} mol^{-1}.

Thermodynamic functions of ANBC(16) were calculated by numerical integration of the present results, and are given in table 3 at rounded temperatures. For the low temperature region, the heat capacity curve was extrapolated smoothly in the calculation.

3.2. *Heat capacity hump in the isotropic liquid phase*

The heat capacity hump appearing in the isotropic liquid has been widely observed in the homologous series of ANBC(n_C) [24]. Similar broad humps have also been reported for some liquid crystalline substances at temperatures above the destruction of a higher order and structure, and the possible assignment of the hump to the destruction of shorter range order than the original unit length has been suggested [27]. In our previous paper [19], the authors pointed out the absence of the hump for an ANBC without the D phase when reporting the growth of the hump with increasing number of the paraffinic carbon atoms in binary systems of an ANBC and *n*-tetradecane. The trend was interpreted by assuming that the hump is due to dissociation of the ANBC dimer and that this process originates the entropy effect. In the present study, the heat capacity curve is discussed qualitatively.

The temperature evolution of the fraction of ANBC(16) molecules participating in dimer formation has been determined from the absorption intensity of the infrared spectra [4]. The fraction decreases by about 10% around the temperature region of the hump. It is known that the enthalpy of formation of a carboxylic acid dimer is roughly equal for most substances with a value of about -60 kJ (mol of dimer)$^{-1}$ [28]. The expected change in enthalpy is thus $0.1 \times 0.5 \times 60$ kJ mol^{-1} = 3 kJ mol^{-1}, comparable with the experimental value 4.65 kJ mol^{-1}. The agreement therefore seems tolerable.

To estimate the contribution of dimer dissociation to the heat capacity, the temperature evolution of the fraction of ANBC(16) molecules participating in dimer formation [4] was fitted to a polynomial. The product of its derivative and the enthalpy difference between monomer and dimer should be a contribution to the heat capacity. The calculated heat capacity curve is compared with the experimental curve in figure 5. Although the peak temperature of the calculated hump, which corresponds to the temperature at the maximum slope of the temperature evolution of the dimer fraction, coincides with the observed feature, the calculated hump is much broader than the experimental one. The fact that the actual hump is confined in a very narrow temperature interval, say 20 K or so, implies the existence of some cooperative mechanism.

3.3. *Phase transitions and excess entropy*

Large supercooling amounting to 20 K and a small degree of superheating were observed in the DSC experiments for the phase transitions from/to the D phase.

Table 3. Standard thermodynamic functions of ANBC(16). The values in parentheses are extrapolated.

T	$C^{\circ}_{p,\mathrm{m}}$	S°_{m}	$[H^{\circ}_{\mathrm{m}}(T)-H^{\circ}_{\mathrm{m}}(0)]/T$	$-[G^{\circ}_{\mathrm{m}}(T)-H^{\circ}_{\mathrm{m}}(0)]/T$
K	J K^{-1} mol^{-1}	J K^{-1} mol^{-1}	J K^{-1} mol^{-1}	J K^{-1} mol^{-1}
10	(6.60)	(2.39)	(1.77)	(0.60)
20	31.82	13.94	9.94	4.00
30	69.38	33.73	23.34	10.39
40	105.52	58.68	39.40	19.29
50	140.5	86.01	56.14	29.87
60	171.6	114.5	72.88	41.6
70	199.8	143.0	88.99	54.0
80	226.1	171.5	104.52	67.0
90	250.6	199.5	119.4	80.1
100	273.2	227.1	133.6	93.4
120	312.7	280.5	160.3	120.2
140	349.5	331.5	184.7	146.8
160	386.3	380.5	207.6	172.9
180	422.5	428.1	229.5	198.7
200	461.2	474.6	250.7	223.9
220	502.9	520.5	271.7	248.8
240	545.2	566.0	292.7	273.4
260	594.1	611.5	313.9	297.6
280	652.9	657.6	335.9	321.7
300	729.1	705.0	359.4	345.6
320	837.6	755.3	385.6	369.7
			transition at 330.19 K	
340	943.5	814.7	420.6	394.1
			transition at 354.43 K	
360	1105	880.7	461.6	419.2
			transition at 369.22 K	
380	991.3	937.3	492.3	445.0
			melting at 401.28 K	
420	1062.9	1137	636.1	501
440	1112	1188	656.6	531
			transition at 445.95 K	
460	1171	1240	679.1	561
			transition at 470.80 K	
			transition at 472.04 K	
480	1581	1306	715.2	591
298.15	719.6	700.6	357.1	343.4

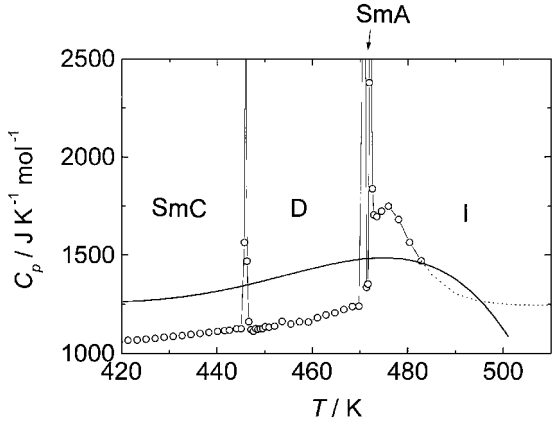

Figure 5. Comparison of the calculated heat capacity arising from the dissociation of the dimers (monotonous solid curve) with the experimental heat capacity. For details of the calculation, see the text.

This suggests that the structural reorganization between the layered structure of the SmC or SmA phase and the structure of the D phase involves a slow complicated process. Supercooling and superheating phenomena are rarely observed in ordinary liquid crystalline substances, except for the transition from mesophase to crystal. It is therefore plausible that the D phase has a structure much different from those of the smectic phases. On the other hand, only a small difference is detected in enthalpy and entropy between the D and the smectic phases. A small enthalpy and entropy of transition between the cubic and SmC mesophases are also found for BABH(8) [20]. In the previous paper [20], the smallness of these values was discussed in terms of curvature elastic (splay) energy, showing that the interwoven jointed-rod model is favourable for the structure of the cubic phase because of cancellation of the splay energy around saddle points. The same argument may apply in the present case.

The study of the binary system between ANBC and *n*-tetradecane clearly showed that the terminal alkoxy chains in the D phase behave like a solvent in lyotropic liquid crystals [19]. The small entropy changes between the SmC, D and SmA phases imply that the dynamical disorder arising from molecular and/or intramolecular motions is similar in each mesophase. A semi-quantitative comparison of the disorder is possible in terms of the excess entropy. Most ANBC(16) molecules are dimerized in the liquid crystalline states and dissociate in the isotropic liquid [4]. An expected entropy of melting due to the molecular core is, therefore, within the range 55–65 $J K^{-1} mol^{-1}$ [29]. The former is the entropy of melting of biphenyl and corresponds with the assumption that all molecules are dissociated, while the latter is the entropy of melting of *p*-quinquephenyl and corresponds to the complete dimerization. As for the terminal chains, it is known that the entropy of melting is a linear increasing function of the number of methylene groups for odd and even *n*-alkanes [30]. The contribution of a methylene group to the entropy of melting is 10.85 $J K^{-1} mol^{-1}$ for the even case and 9.78 $J K^{-1} mol^{-1}$ for the odd case. Since in the present case the chain is not an alkyl but an alkoxy chain, unique identification of either even or odd is hard. The average value 10.31 $J K^{-1} mol^{-1}$ is therefore adopted as the contribution from a methylene group. The terminal methyl group contributes 3.78 $J K^{-1} mol^{-1}$ to the entropy [30]. The contribution of the alkoxy chain is calculated as (158.4 ± 8.0) $J K^{-1} mol^{-1}$, where the error band comes from the use of the average value from the even and odd cases. Together with the contribution from the core, the total sum is estimated as 220 $J K^{-1} mol^{-1}$. The experimental entropy gain is 146.8 $J K^{-1} mol^{-1}$ at the melting temperature and is smaller than the calculated value for the completely disordered model by about 70 $J K^{-1} mol^{-1}$. This indicates that the conformational disordering of the alkoxy chain is incomplete in the mesophases. It is natural to imagine that the methylene groups near to the molecular core retain some order while those far from the core are highly disordered [19]. The difference between the calculated and the experimental entropy gains would reflect such a situation.

Although the experimental entropy gain is smaller than that calculated, the experimental value shows that the alkoxy chains are disordered to a great extent in the liquid crystalline phases. This is indeed necessary for the alkoxy chain to play a role like a solvent [19]. The entropy changes are very small for the transitions between liquid crystalline phases. The entropy gain at the three phase transitions occurring in the solid state is remarkably large, and this trend is also encountered in BABH(8) [20]. It is therefore very likely that the potential disorder might be necessary to stabilize a higher order structure with cubic symmetry formed by long molecules. A similar discussion has been applied to the case of a discotic mesogen [30].

Beyond the existence of cubic liquid crystalline states, there is a further similarity between ANBC and BABH. The constituent molecular particle of the system has a 'doubled' structure in both cases. Although these similarities naturally lead to an expectation that the D phase of ANBC and the cubic phase of BABH are identical, the result from a miscibility test between ANBC(16) and BABH(8) [23] is against this expectation. The two cubic mesogens are immiscible over a wide range of composition. There is, however, no reason why the miscibility rule should be valid in systems where the two constituent molecules are much different in size, as in the present case. In addition, the phase sequence is reversed in these mesogens; the SmC phase is located on the low temperature side of the cubic D phase in ANBC, while it is on the high temperature side of the cubic phase in BABH. The two SmC phases show complete miscibility. In this reversed sequence situation, complete miscibility of the two phases of the components that are identical in nature inevitably requires an immiscibility for the other. The immiscibility cannot therefore be used as evidence for the different nature of two phases separated by a gap. There is another factor seemingly favourable to a violation of the miscibility rule in the present system. The ANBC(16) dimer could be destroyed on mixing with BABH(8) which itself can form hydrogen bonds. Similarly, the higher order structure in the cubic phase of BABH(8) formed by hydrogen bonding in a lateral direction to the molecular axis could be destroyed upon formation of hydrogen bond(s) with ANBC(16). This type of 'structure breaking' would have a significant effect on the cubic phases, resulting in a loss in thermodynamic stability and in the miscibility gap.

4. Conclusion

Heat capacities of ANBC(16) were measured below 500 K by adiabatic calorimetry. Two crystal–crystal phase transitions were discovered at 330.19 and 369.22 K in addition to the known one at 354.43 K. The melting temperature of the pure substance was determined as 401.28 K by the fractional melting method, while the present specimen melted at 401.12 K. All known liquid crystalline phases were clearly detected. The temperatures, enthalpies and entropies of transition were determined for all the phase transitions observed. The standard thermodynamic functions were evaluated at rounded temperatures.

The nature of the heat capacity hump appearing in the isotropic liquid state has been analysed assuming dissociation of ANBC dimers. Although the integrated

enthalpy change is consistent with the mechanism, the shape of the heat capacity curve is insufficiently reproduced, implying the existence of some cooperativity in the phenomenon.

The gain in excess entropy showed the highly disordered conformational states of the terminal alkoxy chains in the liquid crystalline phase. The high disordering of the alkoxy chains is consistent with a behaviour similar to that of a solvent in the cubic phase [19]. The possibility is pointed out that the highly disordered state is necessary for the occurrence of the higher order structure encountered in the cubic phases of ANBC(16) and BABH(8). The small enthalpies of transition between the cubic D and smectic phases are favourable to the interwoven jointed-rod model for the structure of the cubic D phases as far as the curvature elastic energy is concerned.

A logical error is pointed out in relation to any discussion based on the miscibility test that the molecular aggregation or higher order structure must be of different types for the cubic D phase of ANBC(16) and the cubic mesophase of BABH(8). The reason for the immiscibility might arise from the difference in molecular size and/or the 'structure breaking' owing to the different types of hydrogen bonding.

The authors are indebted to Professors Shinichi Yano and Shoichi Kuytsumizu at Gifu University for providing their numerical data for the temperature evolution of the fraction of ANBC(16) molecules participating in dimer formation.

References

[1] Gray, G. W., Jones, B., and Marson, F., 1957, *J. chem. Soc*., 393.
[2] Gray, G. W., and Goodby, J. W., 1984, *Smectic Liquid Crystals—Textures and Structures* (Glasgow and London: Leonard Hill), Chap. 4 and references therein.
[3] Demus, D., Kunicke, G., Neelsen, J., and Sackmann, H., 1968, *Z. Naturforsch*., **23,** 84.
[4] Kutsumizu, S., Kato, R., Yamada, M., and Yano, S., 1998, *J. phys. Chem. B*, **101,** 10 666.
[5] Tansho, M., Onoda, Y., Kato, R., Kutsumizu, S., and Yano, S., 1998, *Liq. Cryst*., **24,** 525.
[6] Diele, S., Brand, P., and Sackmann, H., 1972, *Mol. Cryst. liq. Cryst*., **17,** 163.
[7] Tardieu, A., and Billard, J., 1976, *J. Phys. (Paris) Coll*., **37,** C3-79.
[8] Etherington, G., Leadbetter, A. J., Wang, X. J., Gray, G. W., and Tajbakhsh, A., 1986, *Liq. Cryst*., **1,** 209.
[9] Etherington, G., Langley, A. J., Leadbetter, A. J., and Wang, X. J., 1988, *Liq. Cryst*., **3,** 155.
[10] Levelut, A.-M., and Fang, Y., 1991, *Colloq. Phys*., **23,** C7-229.
[11] Levelut, A.-M., and Clerc, M., 1998, *Liq. Cryst*., **24,** 105.
[12] Luzzati, V., and Spegt, A., 1967, *Nature*, **215,** 701.
[13] Ukleja, P., Siatkowski, R. E., and Neubert, M., 1988, *Phys. Rev. A*, **38,** 4815.
[14] Yamaguchi, T., Yamada, M., Kutsumizu, S., and Yano, S., 1995, *Chem. Phys. Lett*., **240,** 105.
[15] Morimoto, N., Kimura, K., and Sorai, M., 1994, in Proceedings of the 30th Japanese Conference on Calorimetry and Thermal Analysis, Osaka, 1994, 3A14; Morimoto, N., Kimura, K., and Sorai, M., 1995, in Proceedings of the 21st Japanese Conference on Liquid Crystals, Sendai, 1995, 1B15.
[16] Morimoto, N., Kimura, K., Nagano, Y., Saito, K., Morita, Y., Nakasuji, K., and Sorai, M., 1996, in Proceedings of the 14th IUPAC Conference on Chemical Thermodynamics, Osaka, 1996, S6-26 p 17.
[17] Morimoto, N., Nagano, Y., Saito, K., Sorai, M., Morita, Y., and Nakasuji, K., 1997, in Proceedings of the 23rd Japanese Conference on Liquid Crystals, Tokyo, 1997, 3PD10.
[18] Sato, A., Saito, K., and Sorai, M., 1997, in Proceedings of the 23rd Japanese Conference on Liquid Crystals, Tokyo, 1997, 3PD11.
[19] Saito, K., Sato, A., and Sorai, M., 1998, *Liq. Cryst*., **25,** 525.
[20] Morimoto, N., Saito, K., Morita, Y., Nakasuji, K., and Sorai, M., *Liq. Cryst*. (in the press).
[21] Saito, K., Sato, A., Morimoto, N., Yamamura, Y., and Sorai, M. *Mol. Cryst. liq. Cryst*. (in the press).
[22] Schubert, H., Hauschild, J., Demus, D., and Hoffmann, S., 1978, *Z. Chem*., **18,** 256.
[23] Demus, D., Gloza, A., Hartung, H., Hauser, A., Rapthel, I., and Wiegeleben, A., 1981, *Cryst. Res. Technol*., **16,** 1445.
[24] Kutsumizu, S., Yamada, M., and Yano, S., 1994, *Liq. Cryst*., **16,** 1109.
[25] Sorai, M., Kaji, K., and Kaneko, Y., 1992, *J. chem. Thermodyn*., **24,** 167.
[26] Sorai, M., and Seki, S., 1972, *J. phys. Soc. Jpn,* **32,** 282.
[27] Goodby, J. W., Dunmur, D. A., and Collings, P. J., 1995, *Liq. Cryst*., **5,** 703.
[28] Coolidge, A. S., 1928, *J. Am. chem. Soc*., **50,** 2166.
[29] Smith, G. W., 1979, *Mol. Cryst. liq. Cryst*., **49,** 207.
[30] Sorai, M., Tsuji, K., Suga, H., and Seki, S., 1980, *Mol. Cryst. liq. Cryst*., **59,** 33.